https://doi.org/10.5194/egusphere-2026-5689
Preprint. Discussion started: 20 November 2026
© Author(s) 2026. CC BY 4.0 License.

The Seoul Tracer Release Experiment: Investigating Regional Halocarbon Emissions from a Large Metropolitan Area

Michelle J. Müller[1,2], Martin K. Vollmer[1], Stephan Henne[1], Jaegeun Yun[3], Haklim Choi[3], Sunyoung Park[3,4], and Stefan Reimann[1]

[1]Laboratory for Air Pollution / Environmental Technology, Empa, Swiss Federal Laboratories for Materials Science and Technology, Überlandstrasse 129, 8600 Dübendorf, Switzerland
[2]Department of Chemistry and Applied Biosciences, ETH, Swiss Federal Institute of Technology, Zurich, Switzerland
[3]Kyungpook Institute of Oceanography, Kyungpook National University, Daegu 41566, Republic of Korea
[4]Department of Oceanography, Kyungpook National University, Daegu 41566, Republic of Korea

Correspondence: Michelle J. Müller (michellejessy.mueller@empa.ch)

Abstract. Halocarbons have hundreds- to thousands-of-times higher global warming potentials than CO_2, and reducing some of these emissions is part of the Kigali Amendment. Quantifying these emissions at urban and regional scales remains challenging due to uncertainties in emission inventories and observation-based estimates. To constrain hydrofluorocarbon (HFC) emissions in one of Asia's most densely populated areas, a regional-scale experiment was conducted with several deliberate tracer-releases from the Seoul (South Korea) metropolitan area during 2024/2025. The compounds HFC-161 and HFO-1336mzz(E) were released as gaseous tracers under controlled conditions, and their dispersion was tracked along the plume trajectories using measurements from two flask-sampling and one *in-situ*-measurement site. The interpretation of observations was supported by tracer dispersion simulations using the atmospheric transport model FLEXPART. Applying the tracer ratio method, emissions of selected HFCs were determined for the Seoul metropolitan area. They were scaled up to national emissions using population density and then compared with the results of an independent inverse modelling study. The estimates over multiple releases and sites were 2.1±0.6 $\mathrm{kt\,yr^{-1}}$ for HFC-125, 2.0±0.5 $\mathrm{kt\,yr^{-1}}$ for HFC-134a, 0.55±0.1 $\mathrm{kt\,yr^{-1}}$ for HFC-143a, 1.4±0.4 $\mathrm{kt\,yr^{-1}}$ for HFC-152a, and 1.7±0.5 $\mathrm{kt\,yr^{-1}}$ for HFC-32. Our estimates agree with those of an independent inverse modelling study within the combined uncertainties. However, significant sampling-site-specific differences were observed for the various releases, presumably due to limitations in the method's applicability, complex meteorology, and technical challenges during some releases.

1 Introduction

Anthropogenic emissions of chlorine- and bromine-containing halocarbons (used as refrigerants, propellants, industrial processes, and fire repellents), namely (hydro-)chlorofluorocarbons ((H-)CFCs) and halons (H), lead to stratospheric ozone depletion (Molina and Rowland, 1974). These ozone-depleting substances (ODSs) were restricted and phased out from production and consumption for emissive use under the Montreal Protocol (1987) (United Nations, 1987). They were replaced by hydrofluorocarbons (HFCs), which resulted in a rapid increase in these potent greenhouse gases (Liang et al., 2022). A phase-down of

https://doi.org/10.5194/egusphere-2026-5689
Preprint. Discussion started: 20 November 2026
© Author(s) 2026. CC BY 4.0 License.

HFCs was added to the Montreal Protocol by the Kigali Amendment (2016), prompted by these compounds' ability to significantly contribute to global warming (United Nations, 2016). To partially replace these HFCs, low global warming potential (GWP) hydrofluoroolefins (HFOs) are used as a new generation of halogenated compounds.

To monitor compliance with the Montreal Protocol and the progress of the Kigali Amendment, atmospheric observations of gaseous concentrations are beneficial. Two networks that conduct long-term global monitoring are the Advanced Global Atmospheric Gases Experiment (AGAGE, Prinn et al. (2018)) and the National Oceanic and Atmospheric Administration (NOAA, Montzka et al. (2015)). Their globally distributed atmospheric measurements provide information on abundances and trends of halocarbons and, in combination with atmospheric modelling, are used to estimate global, continental, and even national emissions in a so-called top-down approach (Adam et al., 2024; De Longueville et al., 2026; Rust et al., 2022).

Top-down emission estimates based on inverse modelling are well established, but the spatial representativeness of the measurement network is limited with respect to quantifying emissions from individual, small source regions, such as urban areas (Turner et al., 2016). Additional uncertainties in atmospheric transport and boundary layer dynamics arise from different inversion frameworks and transport models (Brunner et al., 2017; De Longueville et al., 2026; Brito Melo, in preparation, 2026). A systematic multi-model and sensitivity study assessed the robustness and uncertainties of inversion estimates and revealed that complex emission distributions in space and time, as well as the choice of the atmospheric transport model, are the main factors influencing differences in and limiting the precision of inverse estimates (Brito Melo, in preparation, 2026). Furthermore, inverse modelling requires continuous atmospheric observations and considerable computational resources, making it less applicable in many world regions.

An alternative top-down approach is the tracer ratio method (TRM), which uses a tracer substance with well-known emissions that is co-emitted with the target gas. The ratio of the above-baseline concentration of the target to the tracer is multiplied by the known emissions of the tracer, resulting in target emission estimates. The TRM assumes co-location and co-variability of tracer and target emissions, and its performance strongly depends on the similarity of their source distributions, particularly in heterogeneous urban environments (Wang et al., 2014). It requires low to no computational work, and no continuous long-term measurements are required, making it more accessible than inverse modelling to estimate regional emissions. Many regional halocarbon TRM emission estimates are based on passive tracers from co-emitted species (e.g., carbon monoxide (Dunse et al., 2005; Rust et al., 2022)), but in complex emission-dense regions, sources vary strongly spatially (poor correlations), and emission inventories of the co-tracers may be inaccurate (Wang et al., 2014). In contrast to relying on passively emitted co-tracers, a regional-scale deliberate-release tracer (DRT) experiment can provide an alternative that eliminates some of these uncertainties, but has not yet been widely applied beyond the facility scale (i.e., for whole metropolitan areas).

One of the first halogenated gases used for deliberate releases (Collins et al., 1965; Turk et al., 1968) was SF_6, as it is non-toxic, dispersible in air, remains chemically unchanged during transport, and is detectable at low concentrations (Maiss et al., 1996). The global increase in the atmosphere through industrial uses and its environmental impact (GWP = 24'700, lifetime = 3200 years, (Burkholder and Hodnebrog, 2022)) make SF_6 less attractive as a DRT (Maiss and Levin, 1994; Maiss and Brenninkmeijer, 1998). However, it was still used for small-scale releases, for example, along SF_5CF_3 to estimate emissions from dairy housings (Mohn et al., 2018). Various cyclic perfluorocarbons (c-PFCs) were also used as DRTs because they had

https://doi.org/10.5194/egusphere-2026-5689
Preprint. Discussion started: 20 November 2026
© Author(s) 2026. CC BY 4.0 License.

low atmospheric baseline concentrations at that time and very low or no pollution events (Simmonds et al., 2002). Multiple DRT experiments were conducted to create validation datasets for atmospheric transport and dispersion models ranging from urban (Draxler, 1985; Cooke et al., 2001) to continental scale (Nodop et al., 1998; Draxler et al., 1991). Recently, ethyl fluoride (HFC-161) was used as a DRT to determine the emissions of a point source of HFC-23 (Rust et al., 2024).

The East Asia region, including Eastern China, Japan, and South Korea, has multiple atmospheric measurement stations or sampling sites used for global, regional, or national top-down emission estimates. For Eastern China, different *in-situ* measurement and flask sampling sites are used to estimate top-down emissions (Stohl et al., 2010; Yao et al., 2012; Yi et al., 2023; Li et al., 2024; Du et al., 2026). Cape Ochi-ishi and Hateruma are halocarbon *in-situ* measurement sites in Japan used for top-down emission estimates (Stohl et al., 2010). However, many regional halocarbon top-down emission estimates are based on the *in-situ* AGAGE measurement station Gosan (GSN) on Jeju Island, South Korea (Stohl et al., 2010; Kim et al., 2012, 2021; Liu et al., 2024; Choi et al., 2024; Choi, in preparation, 2026). A study focusing on the five most abundant HFC, namely HFC-125 (CF_3CHF_2, GWP = 3820), HFC-134a (CF_3CH_2F, GWP = 1330), HFC-143a (CF_3CH_3, GWP = 5900), HFC-152a (CF_2HCH_3, GWP = 153) and HFC-32 (CH_2F_2, GWP = 749), revealed an increase in emissions of these HFCs in the eastern Asia region, especially Eastern China, Japan and South Korea (Burkholder and Hodnebrog, 2022; Choi et al., 2024), in the 2010s. In 2020, Eastern Asia contributed significantly to global HFC emissions (12.6% CO_2-eq. of total CO_2-eq. from the 2022 Ozone assessment Liang et al. (2022)) and to the assumedly unreported global summed HFC emissions (13.1% CO_2-eq. of total unreported CO_2-eq. from the 2022 Ozone assessment Liang et al. (2022)). The regional and national estimates of Choi et al. (2024) were based on long-term atmospheric measurements conducted at GSN and using two independent Bayesian inversion frameworks, FLEXPART-FLEXINVERT+ and NAME-InTEM. The results revealed that most HFC emissions in South Korea originate from the Seoul metropolitan area (SMA) (Choi et al., 2024). Consisting of Seoul, Incheon and Gyeonggi-do, SMA is one of the largest metropolitan areas in Eastern Asia, accounting for approximately half of South Korea's population (Nam and Hong, 2025) and, at least on two sides, is surrounded by regions with low or zero emissions. These criteria make the SMA a suitable testbed for evaluating deliberate regional-scale tracer releases to estimate regional emissions.

In this work, multiple releases of HFC-161 and HFO-1336mzz(E) were conducted in Seoul to estimate the halocarbon emissions from the Seoul Metropolitan Area. Five major HFCs targeted by the Kigali Amendment are assessed: HFC-125, HFC-134a, HFC-143a, HFC-152a, and HFC-32. The results are upscaled to national emissions using population as the scaling factor. To assess the applicability of deliberate regional-scale tracer releases, the national emissions of these five potent greenhouse gases are compared to independent inverse modelling results based on continuous HFC observations from GSN (Choi, in preparation, 2026).

https://doi.org/10.5194/egusphere-2026-5689
Preprint. Discussion started: 20 November 2026
© Author(s) 2026. CC BY 4.0 License.

2 Methodology

2.1 Tracer Ratio Method (TRM)

The tracer ratio method (TRM) is an established technique for estimating regional atmospheric emissions by comparing above-baseline enhancements (pollution) of a target substance with a co-emitted tracer substance with known emissions (Yao et al., 2012; Wang et al., 2014; Rust et al., 2022). The emissions of the target gas (χ), E_χ (in $\mathrm{kt\,yr^{-1}}$), are calculated using (Equ. 1):

$$E_\chi = E_T \cdot \frac{\Delta_\chi}{\Delta_T} \cdot \frac{\mathrm{M}_\chi}{\mathrm{M}_T} \tag{1}$$

where E_T are the known emissions of the tracer, ($\mathrm{kt\,yr^{-1}}$), Δ_χ and Δ_T are the above-baseline concentrations (in ppt) of the target and tracer compound, respectively, and (M) are the respective molar weights (in $\mathrm{g\,mol^{-1}}$).

TRM takes advantage of the similarity in atmospheric behaviour (e.g., dispersion, chemical reactivity, lifetime) and in the origins of the target and tracer emissions.

For a DRT experiment, several criteria concerning the tracer/target relationship should be fulfilled. The target and tracer emissions need to be co-located in space and time. A long dispersion distance allows this co-location requirement to be relaxed, as tracer plumes from a target region/city and a point release will have considerable time to mix in the cross-plume direction. The released tracer amount (release-rate or full amount) should be well quantified. The mole fractions of the target and tracer should be determined in background air before the tracer is released and should remain constant throughout the experiment, in order to maintain a stable target/tracer ratio (atmospheric baseline). Both tracer and target should have similar or negligible atmospheric decay during transport to the measurement site (e.g., atmospheric lifetime). If multiple tracers are used simultaneously, the same contribution of background air should be mixed into the different tracer plumes. No further target or tracer emissions should be added to the air mass during transport. Sampling the tracer plumes at different distances from the source should allow verification that all these criteria are well-met (constant enhancement ratios).

2.2 Error propagation

The uncertainty of the target tracer emissions for an individual event was calculated assuming Gaussian error propagation from Equation 1 and considering additional representativeness uncertainty

$$\sigma^2_{E_x} = E^2_x \left(\frac{\sigma^2_{E_T}}{E^2_T} + \frac{\sigma^2_{\Delta_x}}{\Delta^2_x} + \frac{\sigma^2_{\Delta_T}}{\Delta^2_T} \right) + f^2_{repr}, \tag{2}$$

where f_{repr} is an additional, relative representativeness uncertainty.

The uncertainty of the target tracer enhancement is given by

$$\sigma^2_{\Delta_x} = \sigma^2_{x_{repeat}} + \sigma^2_{x_{bg}} + f^2_{scale,x}\Delta^2_x, \tag{3}$$

where $\sigma_{x_{repeat}}$ is the instrument uncertainty estimated as repeatability from standard gas measurements, $f_{scale,x}$ is the relative scale uncertainty, and the background uncertainty $\sigma_{x_{bg}}$ is taken from the uncertainty estimate of the baseline fit (Sect. 4.2).

https://doi.org/10.5194/egusphere-2026-5689
Preprint. Discussion started: 20 November 2026
© Author(s) 2026. CC BY 4.0 License.

Since the background mole fraction for the reference tracer was indistinguishable from zero, the uncertainty of the reference tracer enhancement is given by

$$\sigma^2_{\Delta_T} = \sigma^2_{T_{repeat}} + f^2_{scale,T}\Delta^2_T. \tag{4}$$

Finally, the uncertainty of the reference tracer release is determined by the uncertainty of the mass flow controller

$$\sigma^2_{E_T} = E^2_T \left(f^2_{\mathrm{MFC,cal}} + f^2_{\mathrm{MFC,rep}}\right), \tag{5}$$

where $f_{\mathrm{MFC,cal}}$ and $f_{\mathrm{MFC,rep}}$ are the relative calibration scale and repeatability uncertainties, respectively. These were assumed to be independent.

Another uncertainty included is the representativeness uncertainty (f_{repr}, Equation 6); more precisely, it represents whether our results rely on SMA or whether additional sources are added along the plume trajectory. For each release, the fraction of SMA air arriving at GSN was determined using a population impact-based FLEXPART simulation (Sect. 4.1, S7). From the sum of all regional fractions f_{r}, f_{SMA} was subtracted resulting in

$$f_{\mathrm{repr}} = \sum_{\text{regions}} f_r - f_{\mathrm{SMA}}. \tag{6}$$

When calculating mean target tracer emissions from several observations, we consider that the individual uncertainties are non-random and, hence, the uncertainty of the mean target tracer emissions is given as the mean over the individual uncertainties.

2.3 Selection of tracers

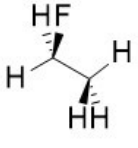
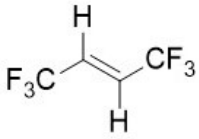
Finding a suitable tracer is challenging because of several tracer-specific criteria. The tracer should be fully volatile under atmospheric conditions, remain in the gas phase in the presence of atmospheric hydrometeors, and exhibit low atmospheric degradability throughout the experiment. The substance should not already be present in the atmosphere, or the concentrations should be distinguishable from those superimposed by the tracer. The tracer should also not be harmful to humans and the environment and should be available for purchase in amounts required for the envisaged transport distance.

Carbon monoxide (CO) is a commonly emitted anthropogenic tracer for estimating regional and national emissions because its atmospheric behaviour and sources are well known. However, it can be difficult to use CO to estimate specific HFC sources due to varying emission source patterns and secondary CO sources (Rust et al., 2022; Pu et al., 2020; Wang et al., 2014; Fang et al., 2012). To circumvent this issue, it is also possible to deliberately release a tracer that is otherwise not emitted in the source region. Previous deliberate tracer releases cover the monitoring of long-range atmospheric transport (Nodop et al., 1998), the evaluation of atmospheric transport models (Simmonds et al., 2021), the evaluation of gas detection and point source quantification methods (Feitz et al., 2018), and the quantification of industrial leaks (Flohr et al., 2021; Maazallahi et al., 2023; Rust et al., 2024).

https://doi.org/10.5194/egusphere-2026-5689
Preprint. Discussion started: 20 November 2026
© Author(s) 2026. CC BY 4.0 License.

Two tracers were deemed suitable for this deliberate release experiment: HFC-161 and HFO-1336mzz(E) (Tab. 1).

Table 1. Properties of HFC-161 and HFO-1336mzz(E) along with their intended use. Unless otherwise referenced, all information is from the Annex of the WMO 2022 Ozone Assessment (Burkholder and Hodnebrog, 2022).

Tracer	HFC-161	HFO-1336mzz(E)
		
IUPAC Name	Fluoroethane	(E)-1,1,1,4,4,4-Hexafluor-2-buten
Chemical Formula	CH_3CH_2F	(E)-$CF_3CH{=}CHCF_3$
CAS	353-36-6	66711-86-2
Molar weight [g mol^{-1}]	48.060	164.05
GWP 100-yr	5	26
Lifetime [days]	80	121
vapour pressures [bar]	9 (25 °C)[a)]	1.6 (20 °C)[b)]
Properties	flammable[c)]	high thermal stability[b)]
Use	refrigerant[c)]	foam blowing agent, specialty gas heat transfer fluid[d)]

a) Chen et al. (2005); Cui et al. (2006), b) Tanaka et al. (2017); Arpagaus et al. (2022), c) Chen et al. (2018); Utage et al. (2021), d) Arpagaus et al. (2022); Bilbao et al. (2024),

HFC-161 was suggested as a potential tracer for small-scale releases in a tracer evaluation study (Simmonds et al., 2021) and was successfully applied during a site-scale release experiment (Rust et al., 2024). For our regional-scale experiment, HFC-161 was chosen as one of the tracers mainly due to its low atmospheric abundance and a sufficiently long atmospheric lifetime of 80 days (Burkholder and Hodnebrog, 2022), allowing us to assume inertness during expected regional transport of a few days. However, the availability of HFC-161 (SynQuest Laboratories, USA) at a competitive price was limited to a leftover stock amount sufficient for about two releases. HFO-1336mzz(E) (Chemours, USA), for which sufficient quantities were available, was selected as a second tracer to complement the experiment. This fluorinated olefin is undetectable in the atmospheric background (unpublished information) and has an atmospheric lifetime of 121 days (Burkholder and Hodnebrog, 2022), hence suitable for our experiment. To our knowledge, neither tracer was produced nor used in South Korea prior to the experiment (See Sec. 3.5).

https://doi.org/10.5194/egusphere-2026-5689
Preprint. Discussion started: 20 November 2026
© Author(s) 2026. CC BY 4.0 License.

3 Deliberate regional-scale tracer release experiment

3.1 Experimental design overview

HFC-161 and HFO-1336mzz(E) were released at Korea University (KU) in Seoul, South Korea, when the forecast showed that the air masses would move south towards the 484 km distant Gosan station (GSN) on Jeju Island (Fig. 1 and Tab. 2) and preferably stay above the ocean during transport. Since 2007, long-term *in-situ* measurements of a wide range of halocarbons have been conducted at the Gosan station. Two additional sites were selected for hourly flask sampling after the releases to cover the large distance between the release point and the *in-situ* measurement location. Coastal Anmyeondo (AMY) is a World Meteorological Organization (WMO) Global Atmosphere Watch (GAW) station located 132 km southwest of Seoul and is used for various greenhouse gas measurements (Lee et al., 2020; Kenea et al., 2026). Mokpo National University (MNU) is 302 km from the release location, near the southwestern end of the mainland. Both flask sampling sites were selected because, in an ideal release scenario, the tracer plume would mostly move over the ocean without additional emissions along the trajectory.

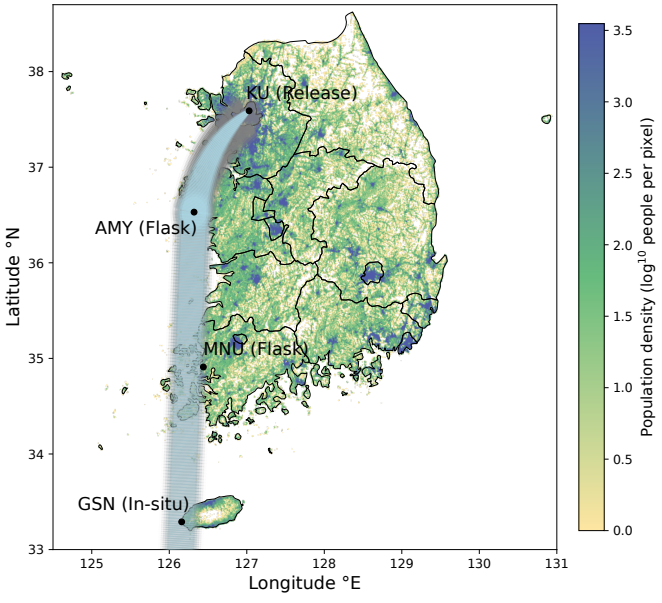


Figure 1. Overview of the desired schematic tracer plume with the release at Korea University (KU), two flask sampling sites at Anmyeondo (AMY) and Mokpo National University (MNU), and the *in-situ* measurement station at Gosan, Jeju Island (GSN). The Seoul metropolitan area (SMA) emission plume is represented in grey, and the released tracer plume in blue. In an ideal release, these schematic plumes are well-mixed at all three sites. The population density is represented at a 1 km resolution and interpolated for the years 2020 to 2024 (Bondarenko et al., 2025). No major population clusters are along the trajectory, so only SMA emissions are expected.

For our experimental setup, negligible HFC emissions are expected from North Korea. A population distribution map (Bondarenko et al., 2025) was used to verify that no emission hotspots are along the trajectory (Fig. 1). For population density, a 1

https://doi.org/10.5194/egusphere-2026-5689
Preprint. Discussion started: 20 November 2026
© Author(s) 2026. CC BY 4.0 License.

km grid was used, and the population of 2020 was extrapolated to 2024 (Bondarenko et al., 2025). The last assumption states that the SMA emissions (grey) and the tracer emissions (blue) are well-mixed at AMY, MNU, and GSN.

Table 2. Location information including the coordinates and distance from the release location.

Locations	Abbreviation	Type	Latitude	Longitude	Outlet/ inlet		Distance
					(a. s. l.)	(a. g. l.)	
Korea University, Seoul	KU	Release	37.59 °N	127.03 °E	71 m	21 m	-
Anmyeondo (GAW Station)	AMY	Flask	36.53 °N	126.32 °E	70 m	40 m	132 km
Mokpo National University	MNU	Flask	34.91 °N	126.44 °E	46.4 m	19.4 m	302 km
Gosan Station, Jeju Island	GSN	*In-situ*	33.29 °N	126.16 °E	72 m	17 m	484 km

3.2 Tracer release setup

For the release location in this complex terrain of the SMA, the Mediheal Earth & Environmental Science Hall of KU (50 m.a.s.l.) was chosen due to its elevated yet central location (Fig. 2). Due to its flammability, the HFC-161 setup was installed on the roof of the 7-story building (71 m.a.s.l.), protected by a semi-permanent shelter. The cylinder containing pure HFC-161 was equipped with a pressure regulator set to 3 bar, a flashback arrestor (WITT Gas, Germany) and a mass flow controller (MFC, 60 $\mathrm{L\,min^{-1}}$ air, Vögtlin Instruments, Switzerland), all connected through 1/4" stainless steel tubing. The cylinder was placed horizontally; it increased the liquid-gas surface area, thereby facilitating the evaporation of the 22 kg of mostly liquid HFC-161. Evaporation rates were predicted based on that surface area, the vapour pressure of HFC-161 (9 bar at 25 °C, Chen et al. (2005)), and the presumed local temperatures (Mackay and van Wesenbeeck, 2014). The MFC was controlled through software (Get Red-y, Vögtlin Instruments, Switzerland), allowing us to control the flow rates through a remotely accessible laptop computer. Unstable release rates during the first releases led to the incorporation of flow tracking software (Red-y meter, Vögtlin Instruments, Switzerland), allowing us to record the release rate at a 30-second interval during the later releases. The MFC was previously calibrated for HFC-161 at Empa (see supplemental information S1).

https://doi.org/10.5194/egusphere-2026-5689
Preprint. Discussion started: 20 November 2026
© Author(s) 2026. CC BY 4.0 License.

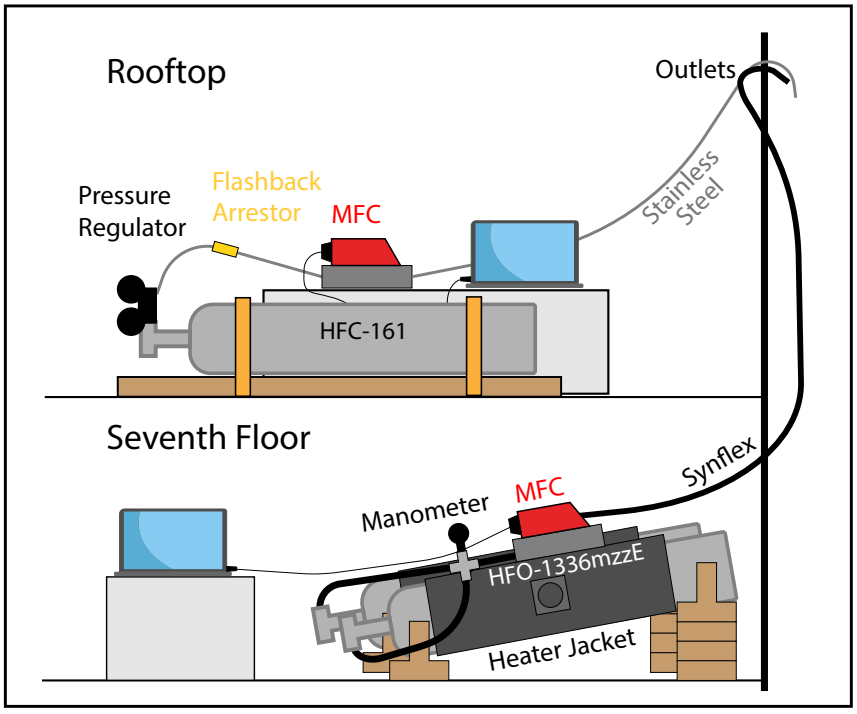


Figure 2. Tracer release setup for HFC-161 (top) and HFO-1336mzz(E) (bottom) at Korea University (KU) in Seoul, South Korea.

The release of HFO-1336mzz(E) was more challenging given its low vapour pressure (1.6 bar at 20 °C, Tanaka et al. (2017)). In addition, the cylinders were equipped with dip tubes, which required a valve-down position (∼20°) to prevent liquid tracer from reaching the MFC (Fig. 2). In order to increase the evaporation rate, the cylinders were paired (later tripled), placed in a temperature-controlled laboratory and heated using gas cylinder heater jackets (Denios, 0–90 °C, Switzerland). These were set to 40–70 °C and powered remotely shortly before the releases. The cylinders were connected using 12 mm Synflex tubing (Eaton, USA) and fed into a single remotely controlled MFC, which was calibrated for HFO-1336mzz(E) in advance (S1). The MFC outlet tubing (12 mm Synflex) was fed through the window and placed next to the HFC-161 outlet on the rooftop.

3.3 Atmospheric transport simulations

In order to predict an ideal time for a tracer release and to support the analysis of the observed plumes, atmospheric transport simulations were carried out with the Lagrangian Particle Dispersion Model (LPDM) FLEXPART (version $9.2_E mpa$, Stohl et al., 2005). Two different atmospheric datasets were used to drive FLEXPART. During forecast mode, global forecast fields of the operational (HRES) Integrate Forecast System (IFS) of the European Centre for Medium range Weather Forecast (ECMWF) were employed. These were available hourly at 0.5° x 0.5° horizontal resolution and were updated four times a day. In hindcast mode, IFS fields were obtained at higher spatial resolution (0.1° x 0.1°), interspersing analysis times with short forecasts.

https://doi.org/10.5194/egusphere-2026-5689
Preprint. Discussion started: 20 November 2026
© Author(s) 2026. CC BY 4.0 License.

In forecast mode, simulations of the emerging tracer plumes were carried out by releasing 50'000 model particles in 3-hourly intervals and following their transport up to 72 hours. These simulations were updated once per day or at a higher frequency when a suitable situation arose. In hindcast mode, the temporal resolution of the simulated releases was increased to every 15 minutes and the number of released model particles to 80'000 per hour, allowing for a more detailed analysis of the tracer plume. Furthermore, the actually observed flow rates of the tracer were taken into account. Resulting concentrations for each 15-minute release were treated separately. Total simulated tracer concentrations were calculated by summation over all releases.

In addition, FLEXPART simulations for the receptor site Gosan were also carried out in time-reversed mode, simulating the surface sensitivity (also called concentration footprint) of air arriving at Gosan. These simulations are done on a regular basis for characterising the Gosan observations and have been available since January 2021, using the same higher-resolution input fields as described above for the hindcast mode.

3.4 Meteorological forecasting and release planning

FLEXPART simulations for Gosan from previous years (2021-2023) were analysed to determine the ideal time of year for the release experiment. FLEXPART-derived source sensitivities for SMA were largest and most frequent from October to April. From these simulations, it was also possible to determine the approximate release strength of the reference tracer required to create a detectable signal at GSN. With a $10\,\mathrm{L\,min^{-1}}$ flow rate of HFC-161, a typical simulated HFC-161 signal of 0.2–0.6 ppt resulted at the GSN station. Taking into account this general range, along with meteorological parameters, MFC flows between 25–60 $\mathrm{L\,min^{-1}}$ for the HFC-161 tracer and 50–120 $\mathrm{L\,min^{-1}}$ for the HFO-1336mzz(E) tracer were used.

The equipment was set up at the beginning of October 2024 and March 2025, respectively. After the equipment was installed, the timing for the release of the tracers, the duration of the release, and the flow rate during the release were determined using the forecasted FLEXPART plumes. When the forecast was promising and the release was started, sampling teams were dispatched to AMY and MNU. For each release, the corresponding FLEXPART forecast can be found in the supplement (S4). After each release, the movement of the tracer plumes was also simulated using FLEXPART (S5).

3.5 Flask sampling and measurement technique

Flask samples were collected at AMY and MNU during several releases. For AMY, the sampling tower line (40 m a. g. l.) was used, and for MNU, the samples were taken on the roof of Engineering Building No.3 (19.4 m a. g. l.). Previously evacuated 6 L stainless steel flasks (Restek, USA) were flushed on site (to ∼3 bar, then vented), through a manifold containing a sampling pump (KNF, Switzerland, N035ANE, fitted with a neoprene membrane) before filling to ∼3.8 bar. A flask was filled every hour during the expected tracer plume passage. Two hours before and after the predicted passage, the flasks were filled to define a non-tracer condition. The flasks were shipped to Empa for analysis.

The flask sample analysis and the *in-situ* measurements were conducted using Medusa GC-MS technology (Miller et al., 2008; Arnold et al., 2012). In the Medusa preconcentration unit, 2 L of air is sampled over a 20 min period at a flow rate of 100 $\mathrm{mL\,min^{-1}}$. The air is dried using two Nafion counter-purge dryers and then concentrated using two trapping steps. The

https://doi.org/10.5194/egusphere-2026-5689
Preprint. Discussion started: 20 November 2026
© Author(s) 2026. CC BY 4.0 License.

traps use HayeSep-D polymer as the adsorbent. After the first trapping step at -165°C, the analytes are transferred by heating to 100 °C to the second trap, which is held at -180°C. Helium (6.0) is used as a carrier gas and to flush out undesired bulk and noble gases (N_2, CO_2, Ar, CH_4). Afterwards, the second trap is heated to 100°C, and the analytes are transferred to the GC (Agilent 6890N) for chromatographic separation using a CP-PoraBOND Q column (0.32 mm internal diameter × 25 m; 5 μm film thickness; Agilent). The separated analytes are then analysed using a quadrupole MS (electron ionisation, selected ion mode, Agilent 5975). To characterise and correct for drifts in the MS sensitivity, air and flask measurements are generally bracketed by whole air working standard measurements. The flask samples collected at AMY and MNU were analysed in triplicate, with a sequence where two flask samples are bracketed by whole air standard measurements. The precisions (1σ std) were 5.3% for HFC-161, 2.4% for HFO-1336mzz(E) and ranged from 0.35–0.56% for the five target HFCs of this study. For the *in-situ* measurements at GSN, measurement precisions were determined from repeated working standard measurements and were 2.9% for HFC-161, 1.0% for HFO-1336mzz(E) and ranged from 0.30–0.83% for target HFCs. During the predicted tracer arrival time at GSN, working standards were measured more sparsely to enhance the air sampling frequency.

Both Medusa GCMSs at Empa and at Gosan are well inter-calibrated using whole air samples compressed into 34 L stainless-steel cylinders (Essex Industries, Inc., USA). For the target HFCs, calibration is conducted through tertiary transfer standards from the AGAGE calibration laboratory at the Scripps Institution of Oceanography (SIO). These tertiary standards are used for weekly calibration of the working standards. The calibration of HFC-161 and HFO-1336mzz(E) is more challenging as these compounds are generally absent in clean whole air. For this reason, all calibration standards of the Empa calibration laboratory are spiked with small quantities of the tracers to generate MS peak signals well suited for quantification and propagation. A transfer standard (E-222) from Empa to GSN allowed for propagation of the tracer calibration to the locally filled working standards, which were also spiked for the duration of the experiment. The primary calibration scales Empa-2013 for HFC-161 and Empa-2016 for HFO-1336mzz(E) are maintained at Empa with estimated accuracies of 10% and 15%, respectively (S2, S2). While the measurements of the two compounds on the Empa laboratory instrument started when the primary calibration scales were established (2013 and 2016, respectively), the measurements on the GSN instrument were introduced in June 2024, five months prior to the first release. This period was used to identify potential emission sources of the two compounds in this region.

4 Tracer releases

The tracer releases were conducted in fall 2024 and spring 2025 (Tab. 3). During the first release on November 18 2024, HFC-161 was released for two hours, followed by an overlapping five-hour release of both tracers, ending with a one-hour release of HFO-1336mzz(E). This staggered release enabled a comparison of the tracer behaviour of the new tracer (HFO-1336mzz(E)) to the previously used HFC-161 tracer (Rust et al., 2024), while extending the release window by a total of three hours. Following the release, eleven flasks were filled at AMY and nine at MNU from 26 to 46 hours after the release started. Both tracers were detected at all locations. On November 22 2024, shortly before disassembling the setup for logistical reasons, the opportunity for a second release arose. Then, only HFO-1336mzz(E) was released and only for three hours, without flask

https://doi.org/10.5194/egusphere-2026-5689
Preprint. Discussion started: 20 November 2026
© Author(s) 2026. CC BY 4.0 License.

sample collection. The tracer plume was detected at GSN. In March 2025, the setup was reassembled at KU, this time with the HFO-1336mzz(E) cylinders connected in triplicate. On April 22, only HFO-1336mzz(E) was released for 7 hours. Flask samples were collected only at MNU due to local PFC pollution at AMY, detected after analysing the flasks taken following the fall release. Small amounts of HFO-1336mzz(E) were detected at MNU and GSN, but for the latter, no clear pollution events were detected for the target HFCs due to generally higher concentrations (S30). The air origin of that release (S34) revealed a large and continuous influence from China, making this release unsuccessful. The last experiment, in May 2025, was used to release all remaining tracer. First, HFC-161 was released for 11 hours, followed by a one-hour break. Then, HFO-1336mzz(E) was released for 5 hours. This staggered release was done to cover a larger time window. No flask samples were taken, and only the HFC-161 tracer was detected at GSN, presumably due to insufficient release amounts of HFO-1336mzz(E). In conclusion, the first release was the most successful in terms of tracer detection and meeting the required tracer transport. Hence, it was used for our most reliable emission estimation. This release will also be used to demonstrate the data processing below.

Table 3. Overview of Releases

Release	Start Date (UTC)	Duration (hours)	Tracer	Amount (kg)	Tracer Detection[a] AMY	MNU	GSN
1	2024-11-18 08:00	7	HFC-161	9.7±0.18	11	9	8
	2024-11-18 10:00	6	HFO-1336mzz(E)	52.1±5.1	11	9	3
2[b]	2024-11-22 06:00	3	HFO-1336mzz(E)	9.6±0.77	-	-	8
3	2025-04-22 06:30	7	HFO-1336mzz(E)	71.1±11.5	-	7	6
4[b]	2025-05-23 18:00	11	HFC-161	11.8±1.8	-	-	1
	2025-05-24 06:00	5	HFO-1336mzz(E)	8.6±1.4	-	-	0

[a] Number of samples where the tracer was detected above a specific threshold (Sect. 4.1).
[b] Leftover tracer was released at suitable times before disassembling the release setup.

4.1 Measurement results and data processing

To isolate the SMA pollution events, the measurements were filtered based on criteria that included a tracer detection threshold, the stability of the target-to-tracer ratio, and air origin. Here, we exemplarily evaluate these criteria for HFC-125 using HFC-161 as a tracer (Fig. 3). For reasons of accuracy and measurement precision, samples with tracer concentrations below a threshold of 0.1 ppt were discarded (grey shading). The second requirement was a stable ratio of target HFC to the tracer to exclude cases of non-SMA emissions added along the flow path. For MNU, such a non-SMA event is indicated in red. In this case, HFC-125 concentrations are declining, then increasing, while the tracer (HFC-161) is continuously declining. For AMY and MNU, the first and last flask samples were filled 2 hours before and after the predicted tracer plume to assess the sampling locations; therefore, these samples are also excluded from analysis. To identify the air masses' origin for the observed samples, FLEXPART simulations using population density as an emission proxy were used (S7). These exclusion criteria were applied to all substances and both tracers separately (S8).

https://doi.org/10.5194/egusphere-2026-5689
Preprint. Discussion started: 20 November 2026
© Author(s) 2026. CC BY 4.0 License.

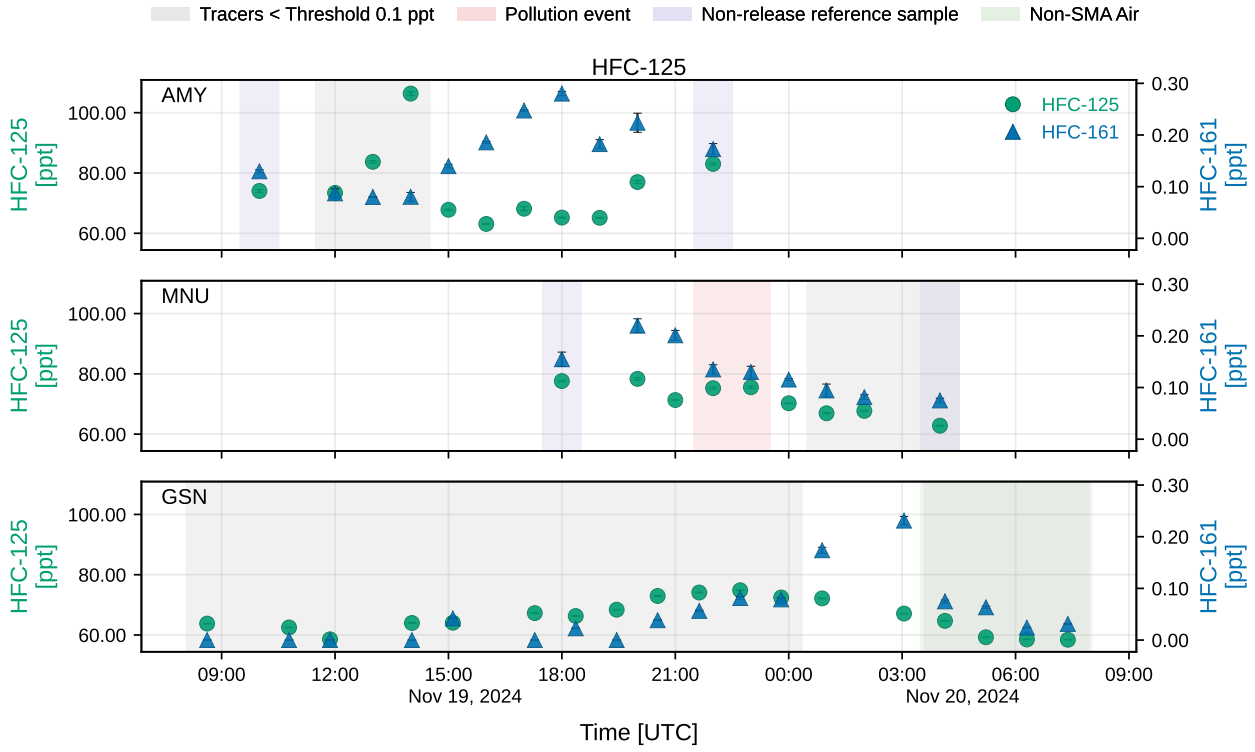


Figure 3. Quality assurance of data from the two flask sampling locations, Anmyeondo (AMY) and Mokpo National University (MNU), and the *in-situ* measurement station Gosan (GSN). The exclusion criteria were a tracer threshold (0.1 ppt, grey), non-SMA pollution events (red), non-release reference flask samples (purple), and air origin based on population-impact FLEXPART simulations (green). HFC-125 (green solid circle) was used as the target compound, and HFC-161 (blue triangle) as the tracer.

4.2 Baseline determination and tracer release rate assignment

To determine what classifies as a pollution event, a baseline concentration must be established for each tracer and target substance. For the tracers, this is rather simple since they were chosen because they are not present at detectable concentrations in the baseline air. Therefore, the baseline for both of them was assumed to be 0 ppt. The baseline of the target gases was determined using the Robust extraction of baseline signals (REBS) method applied to the continuous observations at GSN. REBS is based on robust local regressions and is commonly used to determine baselines of trace gases. REBS only uses residuals below the mode of the residual distribution to estimate the error scale σ to avoid bias from pollution events (Ruckstuhl et al., 2012). Every three hours, a baseline value was determined for the entire GSN time series of the substance and time-matched to the measured data points. The GSN baseline was used for all three locations. The valid above-baseline values were then used for further analysis.

Since the tracer release rates were unstable (Sect. 3.1, S9), an assigned release rate was used to assign a tracer release time and release rate. An example is shown in Figure 4 for HFC-161.

https://doi.org/10.5194/egusphere-2026-5689
Preprint. Discussion started: 20 November 2026
© Author(s) 2026. CC BY 4.0 License.

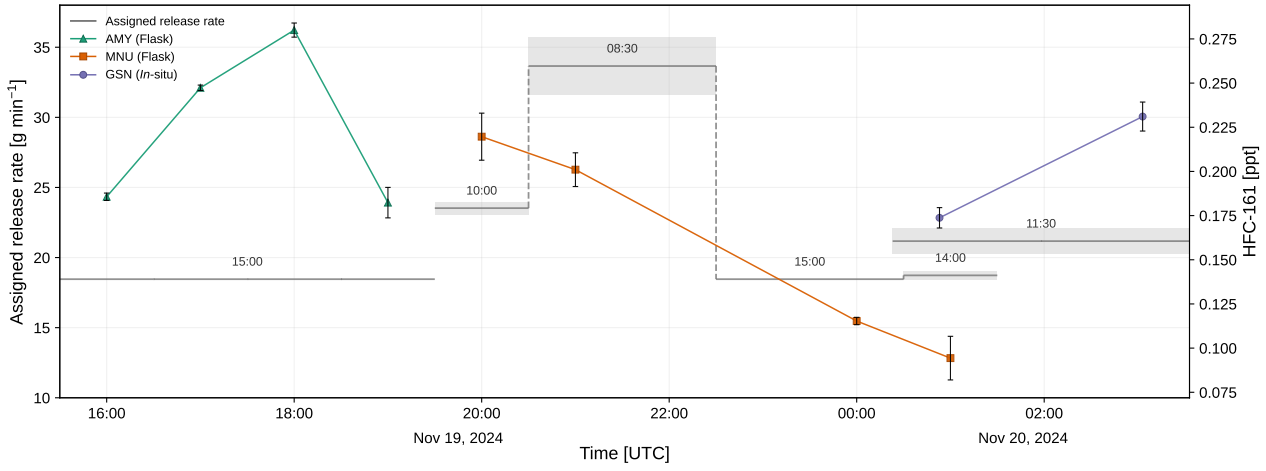


Figure 4. The measured HFC-161 mole fractions in ppt for the flask sampling sites Anmyeondo (AMY, green), Mokpo National University (MNU, orange), and the *in-situ* measurement station Gosan (GSN, purple) and the corresponding assigned release rates of HFC-161 in $\mathrm{g\,min^{-1}}$ (grey). For each measurement, the corresponding tracer release time on November 18, 2024, was assigned using FLEXPART hindcast simulations.

For each measured tracer, the mole fraction was normalised using the time-assigned release rate representative of the sampled air parcel. This assigned release rate was determined from the FLEXPART hindcast simulations. Since the latter resolved the releases at 15-minute intervals, it was possible to associate each sampled air parcel with a release time and hence a flow rate. For this purpose, the FLEXPART release with the largest concentration contribution at the receptor site and given sampling time was selected. Figure 4 shows the tracer normalisation for the November 18, 2024, release. All AMY measurements in green correspond to the release rate at 15:00 UTC, and low uncertainty is observed since the release rate was logged at that time. For MNU, 4 different release rates were assigned with varying uncertainties. For GSN, the same assigned release rate was observed.

4.3 Emission calculation and uncertainties

Equation 7 was used to calculate the SMA emissions for the five target HFCs using either HFC-161 or HFO-1336mzz(E) as a tracer.

$$E_\chi = \frac{\sum_{i=1}^{n} \Delta_{\chi,i}}{\sum_{i=1}^{n} \left(\frac{\Delta_{\mathrm{T},i}}{E_{\mathrm{T},i}} \right)} \cdot \frac{\mathrm{M}_\chi}{\mathrm{M}_\mathrm{T}} \tag{7}$$

For each location and release, the highest observed tracer concentrations $\Delta_{\mathrm{T},i}$ (1-3 measurements in ppt) were selected for analysis. The corresponding above-baseline concentrations of the target HFC ($\Delta_{\chi,i}$ in ppt) were summed up and divided by

https://doi.org/10.5194/egusphere-2026-5689
Preprint. Discussion started: 20 November 2026
© Author(s) 2026. CC BY 4.0 License.

the above-baseline tracer sum, normalised by the assigned release rate $E_{\mathrm{T},i}$ ($\mathrm{g\,min^{-1}}$) normalised above baseline tracer sum. This ratio is then multiplied by the molar ratio ($\frac{\mathrm{M_X}}{\mathrm{M_T}}$), resulting in the target HFC emission E_χ in $\mathrm{g\,min^{-1}}$. Assuming relatively constant emissions from SMA, this estimate can be upscaled to total annual emissions in $\mathrm{kt\,yr^{-1}}$.

As for the uncertainties, for the release on November 18, 2024, the MFC repeatability was 1.1% for HFC-161 and 2.8% for HFO-1336mzz(E), while the MFC calibration uncertainty was 1.9% for HFC-161 and 9.7% for HFO-1336mzz(E). This gives combined release uncertainties of 2.2% and 10.1%, respectively. The representativeness uncertainty for this first release was 23.4% and therefore the largest uncertainty contributor. Over all releases, the release and the representativeness uncertainties remain the major contributors, whereas measurement repeatability and scale uncertainty play a smaller role.

5 Results and discussion

5.1 SMA emission estimates

For the most successful release (November 18, 2024), where both tracers were detected at all three locations, the emission estimates for the five major HFCs are shown in Table 4 based on HFC-161.

Table 4. Seoul metropolitan area (SMA) emission estimates for the November 18, 2024 release derived using HFC-161 as the tracer for the flask sampling sites Anmyeondo (AMY) and Mokpo National University (MNU), and the *in-situ* measurement station Gosan (GSN).

	Compound	AMY	MNU	GSN
HFC emissions	HFC-125	1.1±0.3	3.4±1.0	2.0±0.5
	HFC-134a	0.99±0.3	2.9±0.8	1.7±0.5
	HFC-143a	0.28±0.1	1.4±0.4	0.67±0.2
	HFC-152a	0.71±0.2	2.9±0.9	0.96±0.3
	HFC-32	0.85±0.2	2.4±0.7	1.5±0.4
Tracer	HFO-1336mzz(E)[a]			
	Estimated	54±20	53±20	49±10
	Released[b]	53.2±1	88.0±2	81.5±2

HFC emission estimates are reported in $\mathrm{kt\,yr^{-1}}$ and uncertainties represent 1σ values. [a] HFO-1336mzz(E) is included as a method-validation tracer comparison and is reported in $\mathrm{t\,yr^{-1}}$. [b] Assigned release rate in $\mathrm{g\,min^{-1}}$ upscaled to $\mathrm{t\,yr^{-1}}$ for comparison.

For all five HFCs, significant differences in emission estimates were found when based on the individual sampling sites. AMY resulted in the lowest estimates, followed by GSN and MNU, the latter being three times as high as AMY. These site-specific discrepancies can be partially explained by the complicated plume trajectory and unstable tracer release rates (Sect. 4.2). Although the FLEXPART forecast looked ideal, in the hindcast simulation the tracer plume (Fig. 5, S5) became quite complex the further it moved away from KU, and vertical air mixing and dilution of the tracer may have occurred along

https://doi.org/10.5194/egusphere-2026-5689
Preprint. Discussion started: 20 November 2026
© Author(s) 2026. CC BY 4.0 License.

the transport pathway. The plume reached AMY, still rather compact, and then dispersed along a north-south axis. The southern part of the plume reached MNU, while the northern part passed by AMY again. Shortly after, the southern part reached MNU and finally GSN. The predicted arrival time of the tracer at GSN was 2 hours ahead of the measured arrival (indicated by the onset of measurable tracer concentrations). This temporal difference indicates that the hindcast simulation of the release does not capture the exact tracer transport. For these reasons, the AMY-based estimates were deemed most reliable.

HFC emissions based on the temperature-sensitive HFO-1336mzz(E) were deemed less reliable compared to HFC-161, due to its unstable and poorly quantified release rates. To further explore these uncertain conditions and as a method of validation, HFO-1336mzz(E) was treated as a target gas, and its emissions were calculated using the HFC-161 tracer (Tab. 4). These "*via* HFC-161" results (essentially HFO-1336mzz(E) emissions) were compared to the assigned release rate-based emissions (Sect. 4.2). The two approaches agree for AMY, while for MNU and GSN, the release rate-based emissions are significantly larger (> 60%). We assume that these mismatches for MNU and GSN are related to strongly declining but poorly logged release rates. Hindcast of the release showed that MNU and GSN sampling was mainly capturing the first half of the HFO-1336mzz(E) release. During this time, the release rate dropped untracked to 65%. In contrast, samples that led to the AMY estimates were derived from the second half of the release. The first part was not sampled because the forecasted tracer arrival was considerably later than originally anticipated. At this time, the release rates were frequently logged and more stable, but at a lower magnitude.

The emissions of the five HFCs were also calculated using HFO-1336mzz(E) directly as a tracer (S4). For AMY, the HFC emission estimates compared well with those based on HFC-161 (< 3.6 % for each of the HFCs), a result that is also in agreement with the nearly identical HFO-1336mzz(E) emissions shown in Table 4. As expected, the HFC emission estimates for MNU and GSN differed strongly for the two tracer approaches (S4).

Overall, the observed site- and tracer-discrepancies indicate that both release-rate uncertainties and the complex plume transport contributed to the variability of the emission estimates. As these effects were least pronounced at AMY, the AMY-based estimates are considered the most reliable.

https://doi.org/10.5194/egusphere-2026-5689
Preprint. Discussion started: 20 November 2026
© Author(s) 2026. CC BY 4.0 License.

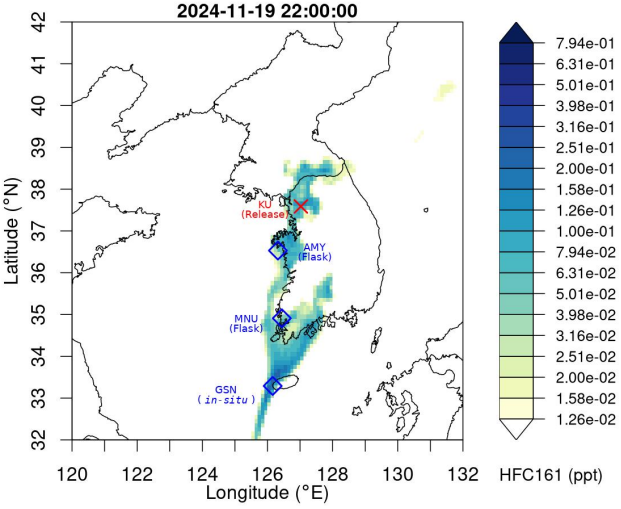


Figure 5. Simulated plume dispersion for the release of HFC-161 on November 18, 2024, 38 hours after the start of the release (November 19, 2024, 22:00 UTC) using FLEXPART.

5.2 Upscaling and comparison with inverse-based top-down national emission estimates

Our target area for emission estimation (SMA) covers a large fraction of the Korean population (∼50 %). We upscaled our SMA HFC emission estimates to Korean national emissions, assuming the same per capita emissions as for the SMA. This assumption of SMA air was supported by population-based air origin simulation (S7).

The most reliable emission estimates, based on AMY using HFC-161 as tracer, result in South Korean national emissions for HFC-125 of $2.1 \pm 0.6\ \mathrm{kt\ yr^{-1}}$, for HFC-134a of $2.0 \pm 0.5\ \mathrm{kt\ yr^{-1}}$, for HFC-143a of $0.55 \pm 0.1\ \mathrm{kt\ yr^{-1}}$, for HFC-152a of $1.4 \pm 0.4\ \mathrm{kt\ yr^{-1}}$, and for HFC-32 of $1.7 \pm 0.5\ \mathrm{kt\ yr^{-1}}$ (Fig. 6). As already noted for the SMA, these estimates agree with the results based on HFO-1336mzz(E), but those for the other two sites (HFC-161-based) are significantly higher. The results for releases 2 and 4 are generally higher than our most reliable result, but most are still within the combined uncertainties of the releases. For the second release, HFC-125 and HFC-32, the two components of R-410A — the most common residential AC refrigerant — are approximately three times as high as the most reliable result, potentially indicating a local source along the trajectory.

https://doi.org/10.5194/egusphere-2026-5689
Preprint. Discussion started: 20 November 2026
© Author(s) 2026. CC BY 4.0 License.

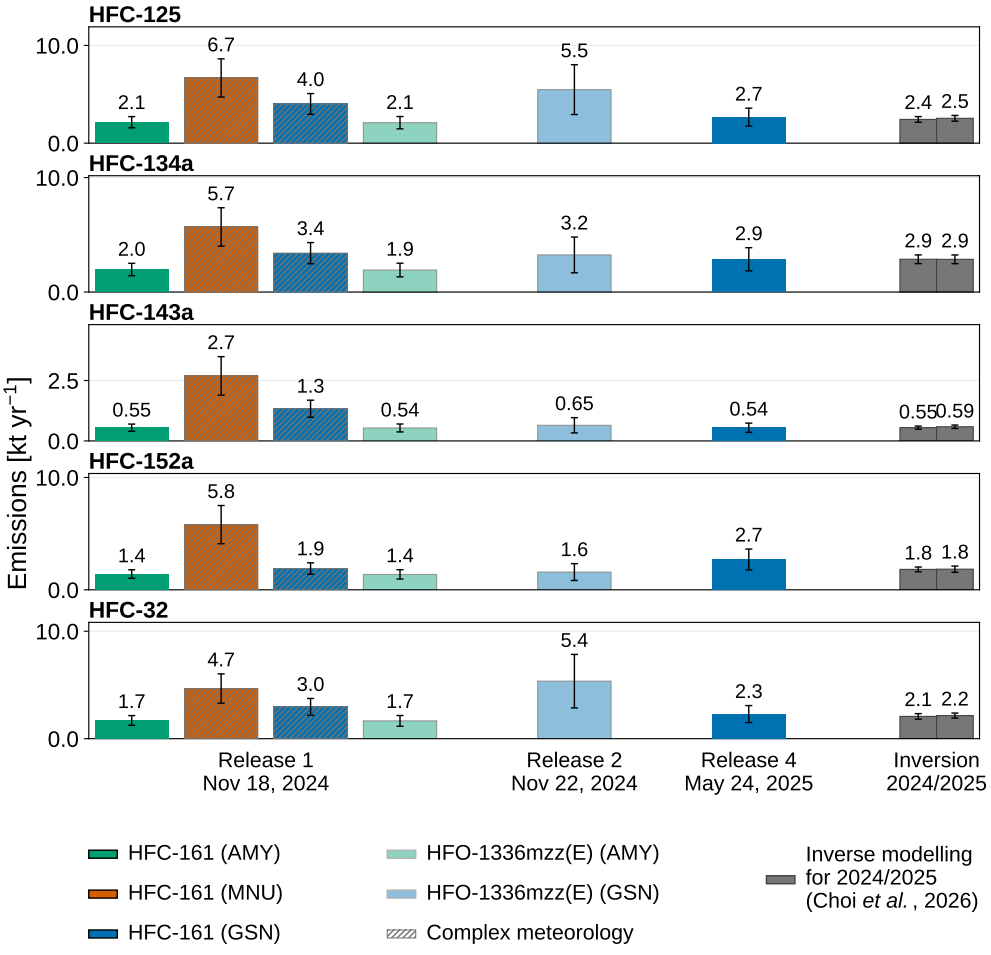


Figure 6. South Korea's national emissions for 2024/2025 based on the tracer ratio method using HFC-161 and HFO-1336mzz(E) as tracers. The emissions for the five HFCs are derived for the flask sampling sites Anmyeondo (AMY) and Mokpo National University (MNU), and the *in-situ* measurement station Gosan (GSN). For the first release (November 18, 2024), the AMY-based emission estimates are in good agreement for both tracers (HFC-161: dark green, HFO-1336mzz(E): light green). As already noted for the SMA, the other two sites (HFC-161-based, MNU: orange, GSN: dark blue) are significantly higher. For the second release (November 22, 2024), only GSN samples (light blue) were used with HFO-1336mzz(E) as a tracer. There, HFC-134a, HFC-143a and HFC-152a are within the combined uncertainties of the most reliable estimates. HFC-125 and HFC-32 were 2.6 and 3.2 times higher than AMY. The last successful release on May 24, 2025, resulted in emission estimates within the combined uncertainties for all five HFCs using HFC-161 as a tracer (dark blue). In comparison to inversion-based results by Choi (in preparation, 2026) (grey), the most reliable results are within the combined uncertainty as well.

In parallel to this experiment, a study applying regional inverse modelling of the eastern Asian region was conducted by Choi (in preparation, 2026). The emissions of the same five target HFCs were estimated for the eastern Asian region and for each country or subregion (Eastern China, Western Japan, and South Korea) for the years 2008 – 2025. Comparing our

https://doi.org/10.5194/egusphere-2026-5689
Preprint. Discussion started: 20 November 2026
© Author(s) 2026. CC BY 4.0 License.

nationally upscaled emission estimates from all successful tracer-release experiments with their estimates for 2024 and 2025 (Fig. 6) showed agreement for the most reliable estimates. The emission estimates for AMY using both tracers are within the uncertainty of the inversion-based mean emission estimates for all five HFCs. This comparison shows that a regional-scale tracer release can be an alternative to inverse modelling, delivering comparable results. However, the setup in terms of distances and the complexity analysis of the release are very important for achieving accurate results.

Furthermore, upscaling our tracer releases, which were a few hours long, to a year also introduces uncertainty due to seasonal variability in target compound emissions. Previous studies in the US indicate a seasonal influence of ∼30% for HFC-134a (Hu et al., 2017; Katharopoulos et al., 2023) and, depending on the emission sector, up to 50% for SF_6 (Hu et al., 2023). However, there are no similar studies in the eastern Asian region to indicate whether the US results are representative of South Korean emissions. In addition, with only 3 valid releases, two in fall 2024 and one in spring 2025, it is beyond this project's scope to determine the seasonality of the five target HFCs and, therefore, the uncertainty in upscaling.

5.3 Methodological limitations and uncertainties

The deliberate regional-scale tracer release method is a promising approach to estimate regional and national emissions. However, this experiment has several methodological limitations and uncertainties. The long transport distance from KU to AMY (132 km), MNU (302 km) and GSN (484 km) allowed a relaxed co-location assumption, where we assumed that our point source (tracer) is spatially co-located with area emissions (SMA). However, the long-distance transport towards GSN was sparse and difficult to track and resulted in low target area representativeness for some releases. Because tracer transport is strongly influenced by meteorological conditions over large distances, reliable forecast and hindcast simulations are essential for release planning, sampling, and interpretation at that scale. For future deliberate tracer release experiments, the sampling distances to the release location should be between 100 and 200 km and ideally in a main downwind direction, assuming there are no major sources along the trajectory. Perpendicular (to the plume) distributed sampling sites could also facilitate plume catching. This setup could result in more frequent releases and more precise plume tracking. Assessing each sampling location before the release in terms of atmospheric baselines, local pollution and emissions along the trajectory is essential in sampling site selection. The importance of maintaining a constant release rate and keeping precise records, especially if a stable release rate is not possible, for accurate emission quantification was highlighted during the first release. Both tracers exhibited some temperature sensitivity during the November releases; however, the low vapour pressure of HFO-1336mzz(E) had a much larger impact on the release-rate stability, making the release-rate characterisation rather difficult. With two releases in fall and two releases in spring, each release represents only the meteorological and emission conditions during a limited time period and therefore may not be representative of annual emissions. Repeated releases under different meteorological conditions and in different seasons would improve the robustness of the emission estimates.

https://doi.org/10.5194/egusphere-2026-5689
Preprint. Discussion started: 20 November 2026
© Author(s) 2026. CC BY 4.0 License.

6 Conclusions

In this work, the feasibility of a deliberate regional-scale tracer release method to estimate regional and national halocarbon emissions was evaluated, using SMA as the study target. Multiple tracer releases in Fall 2024 and Spring 2025 using HFC-161 and HFO-1336mzz(E) as tracers revealed that the results depend strongly on the stability of the release rate and on the meteorological complexity of each release. Samples were taken at three locations, with increasing distance to the release site in Seoul: AMY (flasks, 132 km), MNU (flasks, 302 km), and GSN (*in-situ*, 484 km). Regional emissions were calculated for five HFCs, using the data from all three locations and the two different tracers. These estimated SMA emissions were upscaled based on the population to national emissions and compared to an independent inversion study from the same year. The estimates deemed most reliable from the multiple releases and sites were $2.1 \pm 0.6\ \mathrm{kt\,yr^{-1}}$ for HFC-125, $2.0 \pm 0.5\ \mathrm{kt\,yr^{-1}}$ for HFC-134a, $0.55 \pm 0.1\ \mathrm{kt\,yr^{-1}}$ for HFC-143a, $1.4 \pm 0.4\ \mathrm{kt\,yr^{-1}}$ for HFC-152a, and $1.7 \pm 0.5\ \mathrm{kt\,yr^{-1}}$ for HFC-32. These AMY-based estimates were in agreement within their uncertainty when comparing both tracers to each other (< 3.6 % for each of the HFCs) and to the inversion study (< 34.5 % for each of the HFCs). AMY had the shortest transport distance, and the plume was still rather compact. It was also the least affected by the unstable release rate. Site and tracer instabilities were mainly a result of the complex meteorology and unstable and unquantified release rates. Overall, this study demonstrates that the deliberate regional-scale tracer release method is a viable approach for estimating regional halocarbon emissions. The comparison with independent inversion estimates highlights its potential as a complementary top-down method, while also emphasising the importance of careful tracer selection, release characterisation, and experimental design to obtain robust emission estimates.

Data availability. Numerical data of this study is available under https://zenodo.org/records/24392855 (Müller et al., 2026)

Author contributions. The concept and feasibility of the tracer-release experiment was designed and evaluated by MKV, SP, SR, SH. Experimental setup, sampling, and measurements were performed by MJM, MKV, HC, and YJ; Forecasts, footprints, and inversion results were provided by SH and HC; the article was written by MJM with contributions from MKV and all co-authors.

Competing interests. The authors declare no competing interests.

Acknowledgements. The Halo-CCD project was financed by the Swiss National Science Foundation (SNF) and the National Research Foundation of Korea (NRF). Professor Meehye Lee and her group at the Department of Earth and Environmental Sciences (KU) provided laboratory space for the tracer release setup and local support during the setup. The setup was supported by Myeognjun Oh. The flask samplings were hosted by Sumin Kim in Anmyeondo (AMY) and by Professor Min-Suj Bae at Mokpo National University (MNU). The

https://doi.org/10.5194/egusphere-2026-5689
Preprint. Discussion started: 20 November 2026
© Author(s) 2026. CC BY 4.0 License.

flask samples during the releases were collected with the additional support of Myeognjun Oh, Jihye Jang, and Ji-eun Choi. GSN station is maintained by Jimin Jang. Hans-Rudolf Vollmer crafted the wooden tracer stands, which were essential for the experimental setup. FLEXPART simulations were carried out at the Swiss National Supercomputing Centre (CSCS) under institutional contract ID em05. The Swiss Federal Institute of Metrology (METAS) provided calibration equipment and knowledge for the MFC calibration. OpenAI Codex was used to assist with writing, optimising, and debugging the Python scripts used for data processing, calculations, error analysis, and figure generation. The code was reviewed, and the calculations were manually verified by MJM. MJM takes full responsibility for its integrity. For spelling, grammar, and language improvements, Grammarly, Gemini, and ChatGPT were used.

Financial support. This project is titled Halo-CCD and was funded as a Korean-Swiss Science and Technology Programme Joint Research Projects by the Swiss National Science Foundation (SNF, grant IZKSZ2_218577) and the National Research Foundation of Korea (NRF, grant RS-2023-00229318). FLEXPART simulations were carried out at the Swiss National Supercomputing Centre (CSCS) under institutional contract ID em05.

https://doi.org/10.5194/egusphere-2026-5689
Preprint. Discussion started: 20 November 2026
© Author(s) 2026. CC BY 4.0 License.

References

Adam, B., Western, L., Mühle, J., Choi, H., Krummel, P., O'Doherty, S., Young, D., Stanley, K., Fraser, P., Harth, C., Salameh, P., Weiss, R. F., Prinn, R., Kim, J., Park, H., Park, S., and Rigby, M.: Emissions of HFC-23 do not reflect commitments made under the Kigali Amendment, Communications Earth & Environment, 5, null, https://doi.org/10.1038/s43247-024-01946-y, 2024.

Arnold, T., Mühle, J., Salameh, P. K., Harth, C. M., Ivy, D. J., and Weiss, R. F.: Automated Measurement of Nitrogen Trifluoride in Ambient Air, Anal. Chem., 84, 4798–4804, https://doi.org/10.1021/ac300373e, 2012.

Arpagaus, C., Paranjape, S., Brendel, L., Simoni, L. D., Kontomaris, K., and Bertsch, S. S.: Experimental Investigation of R1336mzz(E) in a High-temperature Heat Pump, in: Proceedings of the International Refrigeration and Air Conditioning Conference, 2289, https://docs.lib.purdue.edu/iracc/2289, 2022.

Bilbao, E., Xia, X., Alonso, M. L., Alonso, R. M., Izcara, J., Izagirre, J., and Lombraña, J. I.: Stability Valorization of Hydrofluoroolefine HFO-1336mzzE and Its Mixtures under Arc Discharge Conditions, Ind. Eng. Chem. Res., 63, 2916–2931, https://doi.org/10.1021/acs.iecr.3c03835, 2024.

Bondarenko, M., Priyatikanto, R., Tejedor-Garavito, N., Zhang, W., McKeen, T., Cunningham, A., Woods, T., Hilton, J., Cihan, D., Nosatiuk, B., Brinkhoff, T., Tatem, A., and Sorichetta, A.: Constrained estimates of 2015–2030 total number of people per grid square at a resolution of 30 arc (approximately 1km at the equator) R2025A version v1, WorldPop, School of Geography and Environmental Science, University of Southampton, https://doi.org/10.5258/SOTON/WP00840, global Demographic Data Project, 2025.

Brito Melo, D. *et al.*: Title to be determined, in preparation, in preparation, 2026.

Brunner, D., Arnold, T., Henne, S., Manning, A., Thompson, R. L., Maione, M., O'Doherty, S., and Reimann, S.: Comparison of four inverse modelling systems applied to the estimation of HFC-125, HFC-134a, and SF_6 emissions over Europe, Atmos. Chem. Phys., 17, 10 651–10 674, https://doi.org/10.5194/acp-17-10651-2017, 2017.

Burkholder, J. B. and Hodnebrog, Ø.: Annex: Summary of Abundances, Lifetimes, ODPs, REs, GWPs, and GTPs, {Appendix} A, Tech. Rep. Report No. 278, World Meteorological Organization, Genéva, https://ozone.unep.org/science/assessment/sap, 2022.

Chen, Q., Hong, R.-h., and Chen, G.-m.: Vapor Pressure Measurements of Ethyl Fluoride, J. Chem. Eng. Data, 50, 1586–1588, https://doi.org/10.1021/je050054u, 2005.

Chen, X., Liu, C., Yang, J., and Chen, J.: Experimental study on R-22, R-427A, R-161 and R-290 in air-source heat pump for space heating at low ambient temperatures, Int. J. Refrig., 96, 147–154, https://doi.org/10.1016/j.ijrefrig.2018.08.021, 2018.

Choi, H., Redington, A. L., Park, H., Kim, J., Thompson, R. L., Mühle, J., Salameh, P. K., Harth, C. M., Weiss, R. F., Manning, A. J., and Park, S.: Revealing the significant acceleration of hydrofluorocarbon (HFC) emissions in eastern Asia through long-term atmospheric observations, Atmos. Chem. Phys., 24, 7309–7330, https://doi.org/10.5194/acp-24-7309-2024, 2024.

Choi, H. *et al.*: Title to be determined, in preparation, in preparation, 2026.

Collins, G. F., Bartlett, F. E., Turk, A., Edmonds, S. M., and Mark, H. L.: A Preliminary Evaluation of Gas Air Tracers, Air Pollut. Control Assoc., 15, 109–112, https://doi.org/10.1080/00022470.1965.10468341, 1965.

Cooke, K. M., Simmonds, P. G., Nickless, G., and Makepeace, A. P. W.: Use of Capillary Gas Chromatography with Negative Ion-Chemical Ionization Mass Spectrometry for the Determination of Perfluorocarbon Tracers in the Atmosphere, Anal. Chem., 73, 4295–4300, https://doi.org/10.1021/ac001253d, 2001.

Cui, X.-l., Chen, G.-m., Han, X.-h., and Wang, Q.: Experimental vapor pressure data and a vapor pressure equation for fluoroethane (HFC-161), Fluid Ph. Equilib., 245, 155–157, https://doi.org/10.1016/j.fluid.2006.04.014, 2006.

https://doi.org/10.5194/egusphere-2026-5689
Preprint. Discussion started: 20 November 2026
© Author(s) 2026. CC BY 4.0 License.

De Longueville, H., Melo, D. B., Redington, A. L., Ramsden, A., Danjou, A., Andrews, P., Pitt, J., Murphy, B., Constantin, L., Stanley, K. M., O'Doherty, S., Wenger, A., Young, D., Engel, A., Schuck, T., Meixner, K., Wagenhaeuser, T., Gad, F., Vollmer, M. K., Reimann, S., Maione, M., Arduini, J., Lunder, C., Schmidtbauer, N., Haszpra, L., Molnár, M., Frumau, A., Couret, C., Rigby, M., Henne, S., Manning, A., and Ganesan, A. L.: European HFC emissions evaluated with multiple atmospheric inverse models and UNFCCC national inventories, Atmos. Chem. Phys., 26, 7647–7675, https://doi.org/10.5194/acp-26-7647-2026, 2026.

Draxler, R. R.: Metropolitan Tracer Experiment (METREX), Tech. Rep. NOAA Technical Memoranda ERL ARL-140, NOAA Air Resources Laboratory, U.S. Department of Commerce, Silver Spring, Maryland, USA, https://repository.library.noaa.gov/view/noaa/9487, 1985.

Draxler, R. R., Dietz, R., Lagomarsino, R. J., and Start, G.: Across North America Tracer Experiment (ANATEX): Sampling and Analysis, Atmos. Environ. Part A, 25, 2815–2836, https://doi.org/10.1016/0960-1686(91)90208-O, 1991.

Du, Q., Hu, X., Zhu, R., Wang, Z., Li, B., Hu, L., Cai, Z., Ji, M., Xu, J., Yu, H., Hu, Y., Yao, B., Pan, X., Liu, L., and Fang, X.: Emissions of fully fluorinated greenhouse gases in central-eastern China inferred from atmospheric observations, J. Environ. Manag., 397, 128 330, https://doi.org/10.1016/j.jenvman.2025.128330, 2026.

Dunse, B. L., Steele, L. P., Wilson, S. R., Fraser, P. J., and Krummel, P. B.: Trace gas emissions from Melbourne, Australia, based on AGAGE observations at Cape Grim, Tasmania, 1995–2000, Atmos. Environ., 39, 6334–6344, https://doi.org/10.1016/j.atmosenv.2005.07.014, 2005.

Fang, X., Wu, J., Su, S., Han, J., Wu, Y., Shi, Y., Wan, D., Sun, X., Zhang, J., and Hu, J.: Estimates of major anthropogenic halocarbon emissions from China based on interspecies correlations, Atmos. Environ., 62, 26–33, https://doi.org/10.1016/j.atmosenv.2012.08.010, 2012.

Feitz, A., Schroder, I., Phillips, F., Coates, T., Negandhi, K., Day, S., Luhar, A., Bhatia, S., Edwards, G., Hrabar, S., Hernandez, E., Wood, B., Naylor, T., Kennedy, M., Hamilton, M., Hatch, M., Malos, J., Kochanek, M., Reid, P., Wilson, J., Deutscher, N., Zegelin, S., Vincent, R., White, S., Ong, C., George, S., Maas, P., Towner, S., Wokker, N., and Griffith, D.: The Ginninderra CH_4 and CO_2 release experiment: An evaluation of gas detection and quantification techniques, Int. J. Greenh. Gas Control, 70, 202–224, https://doi.org/10.1016/j.ijggc.2017.11.018, 2018.

Flohr, A., Matter, J. M., James, R. H., Saw, K., Brown, R., Gros, J., Flude, S., Day, C., Peel, K., Connelly, D., Pearce, C. R., Strong, J. A., Lichtschlag, A., Hillegonds, D. J., Ballentine, C. J., and Tyne, R. L.: Utility of natural and artificial geochemical tracers for leakage monitoring and quantification during an offshore controlled CO_2 release experiment, Int. J. Greenh. Gas Control, 111, 103 421, https://doi.org/10.1016/j.ijggc.2021.103421, 2021.

Hu, L., Montzka, S. A., Lehman, S. J., Godwin, D. S., Miller, B. R., Andrews, A. E., Thoning, K., Miller, J. B., Sweeney, C., Siso, C., Elkins, J. W., Hall, B. D., Mondeel, D. J., Nance, D., Nehrkorn, T., Mountain, M., Fischer, M. L., Biraud, S. C., Chen, H., and Tans, P. P.: Considerable contribution of the Montreal Protocol to declining greenhouse gas emissions from the United States, Geophys. Res. Lett., 44, 8075–8083, https://doi.org/10.1002/2017GL074388, 2017.

Hu, L., Ottinger, D., Bogle, S., Montzka, S. A., DeCola, P. L., Dlugokencky, E., Andrews, A., Thoning, K., Sweeney, C., Dutton, G., Aepli, L., and Crotwell, A.: Declining, seasonal-varying emissions of sulfur hexafluoride from the United States, Atmos. Chem. Phys., 23, 1437–1448, https://doi.org/10.5194/acp-23-1437-2023, 2023.

Katharopoulos, I., Rust, D., Vollmer, M. K., Brunner, D., Reimann, S., O'Doherty, S. J., Young, D., Stanley, K. M., Schuck, T., Arduini, J., Emmenegger, L., and Henne, S.: Impact of transport model resolution and a priori assumptions on inverse modeling of Swiss F-gas emissions, Atmos. Chem. Phys., 23, 14 159–14 186, https://doi.org/10.5194/acp-23-14159-2023, 2023.

https://doi.org/10.5194/egusphere-2026-5689
Preprint. Discussion started: 20 November 2026
© Author(s) 2026. CC BY 4.0 License.

Kenea, S. T., Shin, D., Lee, S., Wang, F., Maksyutov, S., Joo, S., Lee, S., and Kim, S.: Methane (CH_4) emission estimates for South Korea using Lagrangian-based inversion modeling (2010–2021), Atmos. Environ.: X, 30, 100 440, https://doi.org/10.1016/j.aeaoa.2026.100440, 2026.

Kim, J., Li, S., Mühle, J., Stohl, A., Kim, S.-K., Park, S., Park, M.-K., Weiss, R. F., and Kim, K.-R.: Overview of the Findings from Measurements of Halogenated Compounds at Gosan (Jeju Island, Korea) Quantifying Emissions in East Asia, J. Integr. Environ. Sci., 9, 71–80, https://doi.org/10.1080/1943815X.2012.696548, 2012.

Kim, J., Thompson, R., Park, H., Bogle, S., Mühle, J., Park, M.-K., Kim, Y., Harth, C. M., Salameh, P. K., Schmidt, R., Ottinger, D., Park, S., and Weiss, R. F.: Emissions of Tetrafluoromethane (CF_4) and Hexafluoroethane (C_2F_6) From East Asia: 2008 to 2019, J. Geophys. Res. Atmos., 126, https://doi.org/10.1029/2021JD034888, 2021.

Lee, H., Dlugokencky, E. J., Turnbull, J. C., Lee, S., Lehman, S. J., Miller, J. B., Pétron, G., Lim, J.-S., Lee, G.-W., Lee, S.-S., and Park, Y.-S.: Observations of atmospheric $^{14}CO_2$ at Anmyeondo GAW station, South Korea: implications for fossil fuel CO_2 and emission ratios, Atmos. Chem. Phys., 20, 12 033–12 045, https://doi.org/10.5194/acp-20-12033-2020, 2020.

Li, B., Huang, J., Hu, X., Zhang, L., Ma, M., Hu, L., Chen, D., Du, Q., Sun, Y., Cai, Z., Chen, A., Li, X., Feng, R., Prinn, R. G., and Fang, X.: CCl_4 emissions in eastern China during 2021–2022 and exploration of potential new sources, Nat. Commun., 15, 1725, https://doi.org/10.1038/s41467-024-45981-x, 2024.

Liang, Q., Rigby, M., Fang, X., Godwin, D., Mühle, J., Saito, T., Stanley, K. M., Velders, G. J. M., Bernath, P. F., Derek, N., Reimann, S., Simpson, I. J., and Western, L.: Chapter 2: Hydrofluorocarbons (HFCs), in: Scientific Assessment of Ozone Depletion: 2022, Tech. rep., World Meteorological Organization, Genéva, https://ozone.unep.org/science/assessment/sap, 2022.

Liu, Y., Sheng, J., Rigby, M., Ganesan, A., Kim, J., Western, L. M., Mühle, J., Park, S., Park, H., Weiss, R. F., Salameh, P. K., O'Doherty, S., Young, D., Krummel, P. B., Vollmer, M. K., Reimann, S., Lunder, C. R., and Prinn, R. G.: Increases in Global and East Asian Nitrogen Trifluoride (NF_3) Emissions Inferred from Atmospheric Observations, Environ. Sci. Technol., 58, 13 318–13 326, https://doi.org/10.1021/acs.est.4c04507, 2024.

Maazallahi, H., Delre, A., Scheutz, C., Fredenslund, A. M., Schwietzke, S., Denier van der Gon, H., and Röckmann, T.: Intercomparison of detection and quantification methods for methane emissions from the natural gas distribution network in Hamburg, Germany, Atmos. Meas. Tech., 16, 5051–5072, https://doi.org/10.5194/amt-16-5051-2023, 2023.

Mackay, D. and van Wesenbeeck, I.: Correlation of Chemical Evaporation Rate with Vapor Pressure, Environ. Sci. Technol., 48, 10 259–10 263, https://doi.org/10.1021/es5029074, 2014.

Maiss, M. and Brenninkmeijer, C. A. M.: Atmospheric SF_6: Trends, Sources, and Prospects, Environ. Sci. Technol., 32, 3077–3086, https://doi.org/10.1021/es9802807, 1998.

Maiss, M. and Levin, I.: Global increase of SF_6 observed in the atmosphere, Geophys. Res. Lett., 21, 569–572, https://doi.org/10.1029/94GL00179, 1994.

Maiss, M., Steele, L. P., Francey, R. J., Fraser, P. J., Langenfelds, R. L., Trivett, N. B. A., and Levin, I.: Sulfur hexafluoride – a powerful new atmospheric tracer, Atmos. Environ., 30, 1621–1629, https://doi.org/10.1016/1352-2310(95)00425-4, 1996.

Miller, B. R., Weiss, R. F., Salameh, P. K., Tanhua, T., Greally, B. R., Mühle, J., and Simmonds, P. G.: Medusa: A sample preconcentration and GC/MS detector system for in situ measurements of atmospheric trace halocarbons, hydrocarbons, and sulfur compounds, Anal. Chem., 80, 1536–1545, https://doi.org/10.1021/ac702084k, 2008.

https://doi.org/10.5194/egusphere-2026-5689
Preprint. Discussion started: 20 November 2026
© Author(s) 2026. CC BY 4.0 License.

Mohn, J., Zeyer, K., Keck, M., Keller, M., Zähner, M., Poteko, J., Emmenegger, L., and Schrade, S.: A dual tracer ratio method for comparative emission measurements in an experimental dairy housing, Atmos. Environ., 179, 12–22, https://doi.org/10.1016/j.atmosenv.2018.01.057, 2018.

Molina, M. J. and Rowland, F. S.: Stratospheric sink for chlorofluoromethanes: chlorine atom-catalysed destruction of ozone, Nature, 249, 810–812, https://doi.org/10.1038/249810a0, 1974.

Montzka, S. A., McFarland, M., Andersen, S. O., Miller, B. R., Fahey, D. W., Hall, B. D., Hu, L., Siso, C., and Elkins, J. W.: Recent Trends in Global Emissions of Hydrochlorofluorocarbons and Hydrofluorocarbons: Reflecting on the 2007 Adjustments to the Montreal Protocol, J. Phys. Chem., 119, 4439–4449, https://doi.org/10.1021/jp5097376, 2015.

Nam, S. and Hong, S.: The Effects of Employment Center Characteristics on Commuting Time: A Case Study of the Seoul Metropolitan Area, ISPRS International Journal of Geo-Information, 14, 116, https://doi.org/10.3390/ijgi14030116, 2025.

Nodop, K., Connolly, R., and Girardi, F.: The field campaigns of the European Tracer Experiment (ETEX): overview and results, Atmos. Environ., 32, 4095–4108, https://doi.org/10.1016/S1352-2310(98)00190-3, 1998.

Prinn, R. G., Weiss, R. F., Arduini, J., Arnold, T., DeWitt, H. L., Fraser, P. J., Ganesan, A. L., Gasore, J., Harth, C. M., Hermansen, O., Kim, J., Krummel, P. B., Li, S., Loh, Z. M., Lunder, C. R., Maione, M., Manning, A. J., Miller, B. R., Mitrevski, B., Mühle, J., O'Doherty, S., Park, S., Reimann, S., Rigby, M., Saito, T., Salameh, P. K., Schmidt, R., Simmonds, P. G., Steele, L. P., Vollmer, M. K., Wang, R. H., Yao, B., Yokouchi, Y., Young, D., and Zhou, L.: History of chemically and radiatively important atmospheric gases from the Advanced Global Atmospheric Gases Experiment (AGAGE), Earth Syst. Sci. Data, 10, 985–1018, https://doi.org/10.5194/essd-10-985-2018, 2018.

Pu, J., Xu, H., Yao, B., Yu, Y., Jiang, Y., Ma, Q., and Chen, L.: Estimate of Hydrofluorocarbon Emissions for 2012–16 in the Yangtze River Delta, China, Adv. Atmos. Sci., 37, 576–585, https://doi.org/10.1007/s00376-020-9242-3, 2020.

Ruckstuhl, A. F., Henne, S., Reimann, S., Steinbacher, M., Vollmer, M. K., O'Doherty, S., Buchmann, B., and Hueglin, C.: Robust extraction of baseline signal of atmospheric trace species using local regression, Atmos. Meas. Tech., 5, 2613–2624, https://doi.org/10.5194/amt-5-2613-2012, 2012.

Rust, D., Katharopoulos, I., Vollmer, M. K., Henne, S., O'Doherty, S., Say, D., Emmenegger, L., Zenobi, R., and Reimann, S.: Swiss halocarbon emissions for 2019 to 2020 assessed from regional atmospheric observations, Atmos. Chem. Phys., 22, 2447–2466, https://doi.org/10.5194/acp-22-2447-2022, 2022.

Rust, D., Vollmer, M. K., Henne, S., Frumau, A., van den Bulk, P., Hensen, A., Stanley, K. M., Zenobi, R., Emmenegger, L., and Reimann, S.: Effective realization of abatement measures can reduce HFC-23 emissions, Nature, 633, 96–100, https://doi.org/10.1038/s41586-024-07833-y, 2024.

Simmonds, P. G., Greally, B. R., Olivier, S., Nickless, G., Cooke, K. M., and Dietz, R. N.: The background atmospheric concentrations of cyclic perfluorocarbon tracers determined by negative ion-chemical ionization mass spectrometry, Atmos. Environ., 36, 2147–2156, https://doi.org/10.1016/S1352-2310(02)00194-2, 2002.

Simmonds, P. G., Palmer, P. I., Rigby, M., McCulloch, A., O'Doherty, S., and Manning, A. J.: Tracers for evaluating computational models of atmospheric transport and oxidation at regional to global scales, Atmos. Environ., 246, 118 074, https://doi.org/10.1016/j.atmosenv.2020.118074, 2021.

Stohl, A., Forster, C., Frank, A., Seibert, P., and Wotawa, G.: Technical note: The Lagrangian particle dispersion model FLEXPART version 6.2, Atmos. Chem. Phys., 5, 2461–2474, https://doi.org/10.5194/acp-5-2461-2005, 2005.

https://doi.org/10.5194/egusphere-2026-5689
Preprint. Discussion started: 20 November 2026
© Author(s) 2026. CC BY 4.0 License.



Stohl, A., Kim, J., Li, S., O'Doherty, S., Mühle, J., Salameh, P. K., Saito, T., Vollmer, M. K., Wan, D., Weiss, R. F., Yao, B., Yokouchi, Y., and Zhou, L. X.: Hydrochlorofluorocarbon and hydrofluorocarbon emissions in East Asia determined by inverse modeling, Atmos. Chem. Phys., 10, 3545–3560, https://doi.org/10.5194/acp-10-3545-2010, 2010.

Tanaka, K., Ishikawa, J., and Kontomaris, K. K.: Thermodynamic properties of HFO-1336mzz(E) (trans-1,1,1,4,4,4-hexafluoro-2-butene) at saturation conditions, Int. J. Refrig., 82, 283–287, https://doi.org/10.1016/j.ijrefrig.2017.06.012, 2017.

Turk, A., Edmonds, S. M., Mark, H. L., and Collins, G. F.: Sulfur hexafluoride as a gas-air tracer, Environ. Sci. Technol., 2, 44–48, https://doi.org/10.1021/es60013a001, 1968.

Turner, A. J., Shusterman, A. A., McDonald, B. C., Teige, V., Harley, R. A., and Cohen, R. C.: Network design for quantifying urban CO_2 emissions: assessing trade-offs between precision and network density, Atmos. Chem. Phys., 16, 13 465–13 475, https://doi.org/10.5194/acp-16-13465-2016, 2016.

United Nations: Montreal Protocol on Substances That Deplete the Ozone Layer. Montreal, 16 September 1987, Tech. Rep. C.N.263.1987.TREATIES-2 (Depositary Notification), United Nations, New York, 10017, https://ozone.unep.org/treaties/montreal-protocol, 1987.

United Nations: Montreal Protocol on Substances That Deplete the Ozone Layer. Montreal, 16 September 1987. Amendment to the Montreal Protocol on Substances That Deplete the Ozone Layer, Kigali, 15 October 2016, Tech. Rep. C.N.872.2016.TREATIES-XXVII.2.f (Depositary Notification), United Nations, New York, 10017, https://treaties.un.org/doc/Publication/CN/2016/CN.872.2016-Eng.pdf, 2016.

Utage, A. S., Mali, K. V., and Phadake, H. C.: Performance simulation of HFC-161 as an alternative refrigerant to HCFC-22 for room air conditioner, Mater. Today: Proc., 47, 5594–5597, https://doi.org/10.1016/j.matpr.2021.03.474, 2021.

Wang, C., Shao, M., Huang, D., Lu, S., Zeng, L., Hu, M., and Zhang, Q.: Estimating halocarbon emissions using measured ratio relative to tracers in China, Atmos. Environ., 89, 816–826, https://doi.org/10.1016/j.atmosenv.2014.03.025, 2014.

Yao, B., Vollmer, M. K., Zhou, L. X., Henne, S., Reimann, S., Li, P. C., Wenger, A., and Hill, M.: In-situ measurements of atmospheric hydrofluorocarbons (HFCs) and perfluorocarbons (PFCs) at the Shangdianzi regional background station, China, Atmos. Chem. Phys., 12, 10 181–10 193, https://doi.org/10.5194/acp-12-10181-2012, 2012.

Yi, L., An, M., Yu, H., Ma, Z., Xu, L., O'Doherty, S., Rigby, M., Western, L. M., Ganesan, A. L., Zhou, L., Shi, Q., Hu, Y., Yao, B., Xu, W., and Hu, J.: In Situ Observations of Halogenated Gases at the Shangdianzi Background Station and Emission Estimates for Northern China, Environ. Sci. Technol., 57, 7217–7229, https://doi.org/10.1021/acs.est.3c00695, 2023.